Synthesis Using Metal Vapors. Silver Carbonyls. Matrix Infrared, Ultraviolet-Visible, and Electron Spin Resonance Spectra, Structures, and Bonding of $Ag(CO)_3$, $Ag(CO)_2$, Ag(CO), and $Ag_2(CO)_6$

D. McIntosh and G. A. Ozin*

Contribution from the Lash Miller Chemistry Laboratories and Erindale College, University of Toronto, Toronto, Ontario, Canada. *Received June 24, 1975*

Abstract: The heretofore unknown paramagnetic, green complex $Ag(CO)_3$ is synthesized from the cocondensation reaction of silver vapor and carbon monoxide in the temperature range 6–15 K. Characterization of the tricarbonyl complex and support for the mononuclear formulation originate from several sources: (a) mixed $^{12}C^{16}O/^{13}C^{16}O$ and $^{12}C^{16}O/^{12}C^{18}O$ isotopic substitution, frequency and intensity calculations, (b) silver concentration experiments, (c) simultaneous vaporization and cocondensation of Cu and Ag vapors with CO, (d) uv–visible spectroscopy, and (e) ESR spectroscopy. When $Ag(CO)_3$ is synthesized in pure CO, the vibrational data are consistent with a slightly distorted triangular planar structure, towards either C_{2v} or C_2, probably reflecting the low substitutional site symmetry for the molecule in solid CO. However, when synthesized in Ar, Kr, or Xe matrices, $Ag(CO)_3$ appears to adopt a regular, D_{3h}, structure. The ESR spectrum for $Ag(CO)_3$ in CO–Ar matrices supports the contention that the molecule has axial symmetry ($g_\parallel = 2.012$ and $g_\perp = 1.995$). The corresponding uv–visible spectrum is consistent with that expected for a trigonal planar molecule having a $^2A_2''$ electronic ground state which is compatible with the observed blue shifts for all of the optical transitions of $Ag(CO)_3$ compared to $Cu(CO)_3$. Unlike the corresponding copper vapor–carbon monoxide reaction, $Ag_2(CO)_6$ could not be synthesized from the matrix reaction of Ag and CO at high concentrations of silver. However, $Ag(CO)_3$ is found to be thermally and photochemically labile in pure CO. During warm-up experiments in the range 20–35 K, $Ag(CO)_3$ undergoes a facile dimerization reaction to form $Ag_2(CO)_6$. On the other hand, warm-up experiments performed on $Ag(CO)_3$ in Kr and Xe matrices demonstrate that the molecule is stable up to at least 80–100 K. Under these conditions, $Ag(CO)_3$ shows no tendency to decompose or dimerize. The thermal behavior of $Ag(CO)_3$ is taken to indicate that some kind of matrix-assisted diffusion process is operating in pure CO. Possible diffusion mechanisms are discussed in the light of recent matrix kinetic studies of the dimerization reaction of $Ag(CO)_3$ in pure CO. Using methods similar to those outlined for $Ag(CO)_3$, the synthesis and characterization of the $Ag(CO)_2$ and Ag(CO) complexes in Ar, Kr, and Xe are described. The information extracted from the infrared and uv–visible spectra of the complete series of complexes $M(CO)_n$ (where M = Cu or Ag; $n = 1$–3) is used to draw conclusions about their molecular and electronic structures, thermodynamic stabilities, and bonding properties. Of special interest is the anomalous behavior observed for the Cotton–Kraihanzel CO bond stretching force constants. A rationalization in terms of a very stable nd^{10} valence shell and the participation of energetically accessible valence p_π metal orbitals in the overall bonding scheme are presented. In this context, the role of p_π metal orbitals in the recently synthesized main group carbonyl complexes of Al, Ga, Ge, and Sn is assessed as is the interesting relationship between the $M(CO)_n$ data (where M = Cu or Ag, $n = 1$–3) and those for CO chemisorbed onto Cu and Ag metallic films. Finally, the matrix-induced frequency shifts for $Ag(CO)_n$ in Ar, Kr, and Xe are rationalized in terms of Buckingham's theory of nonspecific solute–solvent interactions.

The state of knowledge of the carbonyl chemistry of silver has remained essentially unchanged since the early reports of failure in 1866.[1] Up to the present time no stable carbonyl nor carbonyl derivative of silver has been reported and until very recently the only available information pertaining to Ag–CO bonds was restricted to CO chemisorbed onto silver films.[2]

In this paper we report the details of the silver vapor–carbon monoxide reaction, the products of which are proven to be $Ag(CO)_3$, $Ag(CO)_2$, Ag(CO), and $Ag_2(CO)_6$. Methods comparable to those used in studying the Cu–CO system have been applied.[3-6]

Experimental Section

Monatomic Ag was generated either by directly heating a thin tantalum rod (0.025 in.) around the center of which was wound silver wire (0.005 in.) or by directly heating a tantalum Knudsen cell (wall thickness 0.015 in., orifice diameter 0.010–0.020 in.), the silver being contained in a boron–nitride liner (wall thickness 0.010 in.). The silver metal (99.99%) was supplied by Imperial Smelting Co., Toronto. Research grade $^{12}C^{16}O$ (99.99%) was supplied by Matheson of Canada and $^{12}C^{16}O/^{13}C^{16}O$, $^{12}C^{16}O/^{12}C^{18}O$ isotopic mixtures by Stohler, Montreal. The furnace used for the evaporation of the metals has been described previously.[8] The rate of metal atom deposition was continuously monitored using a quartz crystal microbalance.[9] To obtain quantitative data for Ag/CO and Ag/CO/M (M = Ar, Kr, or Xe) cocondensations, it was necessary to calibrate carefully the rate of deposition of both metal and gas onto the sample window as described previously.[10] In the infrared experiments, matrices were deposited on either a NaCl or a CsI plate cooled to 10–12 K by means of an Air Products Displex closed-cycle helium refrigerator or to 6 K by a liquid helium transfer system. Spectra were recorded on a Perkin-Elmer 180 spectrophotometer. Uv–visible spectra were recorded on a standard Unicam S.P. 8000 instrument in the range 190–700 nm, the sample being deposited onto a LiF or NaCl optical plate cooled to 6–8 K. In the ESR experiments, the sample was deposited onto a sapphire rod (dimensions $1.75 \times 0.12 \times 0.04$ in.) cooled to 6 K. Using a specially designed telescopic vacuum shroud[11] the sample could be lowered into an extension quartz tailpiece, held in the microwave cavity of a standard Varian E 4 spectrometer. ESR spectra were recorded in the range 0–6000 G with microwave powers varied between 0.1 and 10 mW for optimum resolution conditions.

Silver Tricarbonyl, $Ag(CO)_3$

Matrix Reactions of Silver Vapor with Pure CO; Infrared Experiments. When silver vapor (which is greater than 99% monatomic[12]) is cocondensed with pure $^{12}C^{16}O$ at 10–12 K and under concentration conditions which favor the formation of mononuclear reaction products ($Ag:CO \leq 1:10^4$), the infrared spectrum shown in Figure 1 is obtained after about 1 h. The spectrum is relatively simple, displaying an intense doublet at 1967/1937 (I_2/I_3) cm^{-1} together with a very much weaker line at about 2085 (I_1) cm^{-1} (seen as a shoulder on the natural abundance $^{12}C^{18}O/^{13}C^{16}O$ isotopic doublet at cm^{-1}) in the CO stretching region. Only when the 1967–1937 cm^{-1} doublet was arranged to be fully absorbing was it possible to observe a very weak, broad line at about 250 cm^{-1} which might be attributable to a Ag–C skeletal stretching mode (see later).

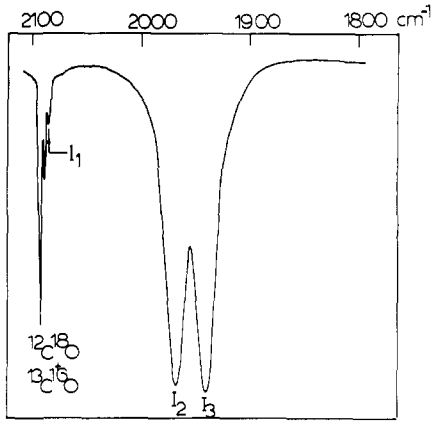

Figure 1. The matrix infrared spectrum in the CO stretching region obtained by cocondensing silver vapor with $^{12}C^{16}O$ at 12 K ($I_{1,2,3}$ depict the ν(CO) stretching modes of $Ag(CO)_3$—see text).

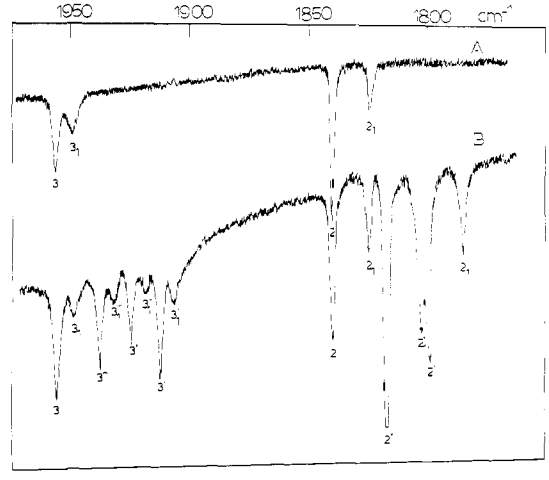

Figure 2. The matrix infrared spectrum of the products of the cocondensation reaction of Ag atoms with (A) $^{12}C^{16}O/Ar \simeq 1/100$ and (B) $^{12}C^{16}O/^{12}C^{18}O/Ar \simeq 1/1/250$ matrices at 10–12 K showing $Ag(CO)_3$ and $Ag(CO)_2$ (where 2 and 3 = site 1; 2_1 and 3_1 = site 2).

Early on in these infrared experiments, it was discovered that the product of the Ag–CO reaction was extremely sensitive to the radiation emitted from the Nernst glower of the infrared spectrometer and could be observed to decompose slowly (see later) in the beam. This photochemical lability became particularly noticeable during warm-up experiments at temperatures above 12 K. The placement of a germanium UV-visible-cutout filter between the source and sample was found to be sufficient to eliminate completely this photochemical complication.

The infrared spectrum obtained for the product of the Ag–CO reaction resembles very closely that previously observed for the analogous Cu–CO reaction,[5] the product of which has been established to be $Cu(CO)_3$. A similar doublet splitting in the CO stretching region was also observed for $Cu(CO)_3$ at 1990.0 and 1976.8 cm^{-1} and was proven to originate from the removal of the degeneracy of the E′ νCO mode of a planar D_{3h} molecule, because of the low C_2 substitutional site symmetry found for the molecule in solid CO.

The warm-up behavior for the product of the Ag/CO reaction is also similar to that observed for $Cu(CO)_3$, namely, a gradual decrease in the intensity of the CO stretching modes at 2085, 1967, and 1937 cm^{-1} (the three lines maintaining constant relative intensities) simultaneous with the growth and eventual decay of two sets of new lines at 1998, 1955 cm^{-1} and 1980, 1944 cm^{-1} (see Figure 1 ref 41). This behavior can be qualitatively explained by a model in which $Ag(CO)_3$ dimerizes to form the Ag–Ag bonded dimer $Ag_2(CO)_6$ which then decomposes to give other products, perhaps Ag_2 and CO. Support for this proposal stems from matrix kinetic experiments (see part II of this paper (ref 41) for further details).

Further evidence that supports the mononuclear formulation of the tricarbonyl stems from *five* other sources listed below, each of which will be elaborated on in turn. (a) Besides the tricarbonyl, two other mononuclear carbonyls, $Ag(CO)_2$ and Ag(CO), can be synthesized in dilute CO/Ar, CO/Kr, and CO/Xe matrices, which after warm-up revert to the proposed tricarbonyl, $Ag(CO)_3$, which is further supported by (b) matrix infrared $^{12}C^{16}O/^{13}C^{16}O$ isotopic frequency and intensity data, (c) silver concentration studies, (d) matrix uv-visible spectroscopy, and (e) matrix ESR spectroscopy.

Infrared Experiments for $Ag(CO)_3$ in Ar, Kr, and Xe Matrices. When Ag atoms were cocondensed with CO/Ar $\simeq$ 1/1000 matrices at 10–12 K at *low* silver concentrations, a typical spectrum obtained after deposition is shown in Figure 2A. On warming the matrix to 35–40 K, the low frequency (1842/1827.5 cm^{-1}) CO stretching modes gradually decrease in intensity (discussed later), leaving a band[13] at 1958.2 cm^{-1} which can be associated with the complex of highest stoichiometry and whose frequency (taking into account matrix shifts of about 5 cm^{-1}) is roughly the mean of the 1967/1937-cm^{-1} doublet observed in pure CO (previous section). Apart from small matrix frequency shifts which will be discussed in detail in a later section, essentially identical spectra were obtained when Ag atoms were cocondensed with CO/Kr $\simeq$ 1/80 and CO/Xe $\simeq$ 1/20 matrices which after warm-up led to a single species absorbing at 1932.8 (Kr) and 1926.3 (Xe) cm^{-1}.

That the lines at 1958.2, 1932.8, and 1926.3 cm^{-1} in Ar, Kr, and Xe matrices, respectively, can all be associated with one and the same molecular species was established from $^{12}C^{16}O/^{13}C^{16}O/M$ and $^{12}C^{16}O/^{12}C^{18}O/M$ (where M = Ar, Kr, or Xe) mixed isotope experiments (see for example Figure 3), each of which produced an infrared spectrum consisting of three new lines below the mode observed in $^{12}C^{16}O/M$ (Table I) characteristic of a tricarbonyl containing three equivalent carbonyl groups. The matrix splitting alluded to earlier for this species in Ar is confirmed by the mixed $^{12}C^{16}O/^{12}C^{18}O/Ar$ experiments (Figure 2B), which reveal that each component of the original doublet in $^{12}C^{16}O/Ar$ matrices produces an associated "quartet" isotope pattern in $^{12}C^{16}O/^{12}C^{18}O/Ar$, expected for a tricarbonyl molecule experiencing two slightly different matrix environments.

Mixed $^{12}C^{16}O/^{13}C^{16}O$ Experiments. Having established that the species of highest stoichiometry in Ar, Kr, and Xe matrices is most likely a mononuclear tricarbonyl, we can now return to the interesting problem of the 30-cm^{-1} doublet splitting observed for this species in pure CO matrices. Unfortunately, the situation in CO matrices is not quite as straightforward as in the noble gas matrices, mainly on account of the band widths of the CO stretching modes (~9–10 cm^{-1}) which, when taken together with the 30-cm^{-1} doublet splitting, lead to the inevitability of band overlap in $^{12}C^{16}O/^{13}C^{16}O$ mixed isotope experiments. With these complications in mind, the infrared spectrum obtained on cocondensing Ag atoms with $^{12}C^{16}O/^{13}C^{16}O$ mixtures at 10 K at low silver concentrations is listed in Table II. As anticipated, the spectrum is complex but nevertheless can be roughly resolved into a *nine*-line pattern, which is that expected for a triangular planar $Ag(CO)_3$ molecule (Table II) which has experienced either a C_{2v} or C_2 lattice distortion, a situation reminiscent of $Cu(CO)_3$ in pure CO.[5]

Isotopic Frequency and Intensity Calculations for Silver Tricarbonyl in Ar, Kr, and Xe Matrices. The frequency and intensity calculations of the $^{12}C^{16}O/^{13}C^{16}O/M$ (where M = Ar, Kr, and Xe) mixed isotopic data are greatly simplified if one assumes the Cotton–Kraihanzel approximation.[14] Since

Table I. Observed and Calculated Frequencies and Intensities of Isotopic $Ag(^{12}C^{16}O)_n(^{12}C^{18}O)_{3-n}$ or $Ag(^{12}C^{16}O)_n(^{13}C^{16}O)_{3-n}$ (where n = 0–3) in Ar (Both Sites Included), Kr, and Xe Matrices

Obsd freq	Calcd freq	Obsd intens	Calcd intens	Assignment[c]
		Argon (site 3)[a]		
1912.2	1911.8	8.54	9.03	(IV) (E′); (III) (B_1)
1925.1	1923.9	5.40	5.40	(II) (A_1)
1937.8	1938.6	6.70	5.31	(III) (A_1)
1958.2	1959.0	10.00	10.00	(I) (E′); (II) (B_1)
	f_r = 16.19; f_{rr} = 0.69 mdyn/Å			
		Argon (site 3_1)[a]		
1908.2	1906.3	8.26	8.83	(IV) (E′); (III) (B_1)
1918.9	1918.0	5.95	5.31	(II) (A_1)
1935.5	1932.5	5.97	5.40	(III) (A_1)
1951.8	1953.4	10.00	10.00	(I) (E′); (II) (B_1)
	f_r = 16.02; f_{rr} = 0.61 mdyn/Å			
		Krypton[a]		
1887.2	1886.8	8.90	9.14	(IV) (E′); (III) (B_1)
1901.0	1900.0	6.81	5.54	(II) (A_1)
1914.4	1915.1	6.63	5.55	(III) (A_1)
1932.8	1933.4	10.00	10.00	(I) (E′); (II) (B_1)
	f_r = 16.20; f_{rr} = 0.89 mdyn/Å			
		Xenon[b]		
1883.5	1883.5	9.83	9.56	(IV) (E′); (III) (B_1)
1895.1	1894.8	6.88	5.70	(II) (A_1)
1908.0	1908.3	6.32	5.68	(III) (A_1)
1926.3	1926.4	10.00	10.00	(I) (E′); (II) (B_1)
	f_r = 15.66; f_{rr} = 0.67 mdyn/Å			

[a] $^{12}C^{16}O/^{13}C^{16}O$ used with ratio ~1.05. [b] $^{12}C^{16}O/^{12}C^{18}O$ used with ratio ~1.00. [c] Assignment notation: (I) = $Ag(^{12}C^{16}O)_3$; (II) = $Ag(^{12}C^{16}O)_2(^{13}C^{16}O)$ or $Ag(^{12}C^{16}O)_2(^{12}C^{18}O)$; (III) = $Ag(^{12}C^{16}O)(^{13}C^{16}O)_2$ or $Ag(^{12}C^{16}O)(^{12}C^{18}O)_2$; (IV) = $Ag(^{13}C^{16}O)_3$ or $Ag(^{12}C^{18}O)_3$.

Table II. Observed and Calculated Frequencies of Isotopic $Ag(^{12}C^{16}O)_n(^{13}C^{16}O)_{3-n}$ (where n = 0–3) in Solid $^{12}C^{16}O/^{13}C^{16}O$

Calcd[a] (cm^{-1})	Obsd (cm^{-1})	Assignment[c]
1896.8	1897.6	(IV) B_1; (VI) B_1
1909.5	1905.4	(V) A′
1911.5	1915.6	(III) A′
1924.0	1927.8	(VI) A_1
1936.3	1934.8	(II) A_1; (V) A′
1939.9	1939.2	(I) B_1; (II) B_1
1946.0	1946.0	(IV) A_1
1963.2	1960.0	(III) A′
1967.7	1968.8	(I) A_1
2058.0	*b*	(I) A_1
2045.7	*b*	(II) A_1
2046.9	*b*	(III) A′
2034.7	*b*	(IV) A_1
2031.2	*b*	(V) A′
2012.3	*b*	(VI) A_1

[a] Best fit force constants: f_r = 15.89, f_r' = 16.18, f_{rr} = 0.69, f_{rr}' = 0.50 mdyn/Å. [b] Low intensity, high frequency isotope lines not observed. [c] See H. Huber, E. P. Kundig, M. Moskovits, and G. A. Ozin, *J. Am. Chem. Soc.*, **95**, 332 (1975), for notation.

$Ag(CO)_3$ occurs in two sites (3 and 3_1) in Ar matrices, calculations based on D_{3h} symmetry were performed on both sites. In Kr and Xe, only single site calculations were necessary. The frequencies and intensities were computed using methods similar to those delineated for $Cu(CO)_3$[5] and yielded the set of data shown in Table I. The agreement between the observed and calculated values for all observed CO stretching modes in Ar, Kr, and Xe matrices is excellent and provides convincing evidence for the correctness of the mononuclear D_{3h} $Ag(CO)_3$ structural assignment.

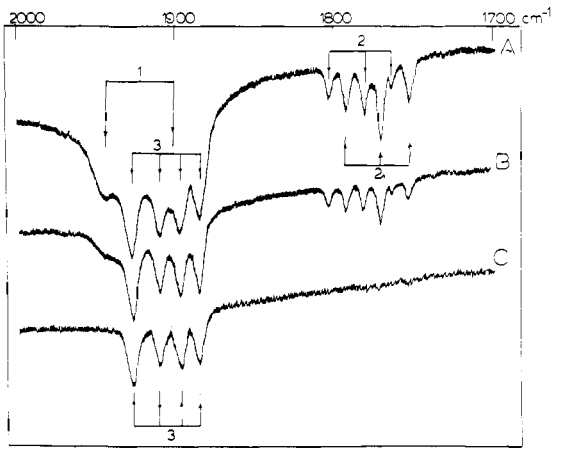

Figure 3. The matrix infrared spectrum of the products of the cocondensation reaction of Ag atoms with $^{12}C^{16}O/^{13}C^{16}O/Xe \simeq 1/1/40$ matrices (A–C) after warm-up to 45, 60, and 85 K, showing the isotope patterns of $Ag(^{12}C^{16}O)_n(^{13}C^{16}O)_{m-n}$ where m = 3, n = 0–3; m = 2, n = 0–2; and m = 1, n = 0–1 and 2 refers to site 1 and 2_1 refers to site 2 of the dicarbonyl (see text).

Silver Tricarbonyl in Solid Carbon Monoxide. The doublet splitting observed for $Ag(CO)_3$ in solid CO (Figure 1) suggests that the formally D_{3h} planar molecule in Ar, Kr, and Xe matrices does not retain its threefold axis of symmetry in pure CO. Inspection of the CO lattice indicates a C_2 site perturbation arising from the inclination of the CO molecules to the $Ag(CO)_3$ molecular plane. Hence the infrared active E′ νCO stretching mode is split into two components, A (I_2) and B (I_3), under C_2 symmetry and the A_1' νCO stretching mode becomes weakly infrared active A (I_1). On the basis of this model, the following intensity expression can be readily derived:

$$\frac{I_1 + I_2}{I_3} = \frac{1 + 2\cos^2 \alpha/2}{2\sin^2 \alpha/2}$$

where

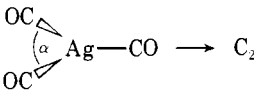

From the observed value of the ratio

$$\frac{I_{2085} + I_{1967}}{I_{1937}} = \frac{0.03 + 0.71}{0.93} = 0.796$$

one calculates $\alpha \simeq 132°$.

Further support for the C_2 distortion of the $Ag(CO)_3$ molecule in CO matrices was obtained from mixed isotopic substitution experiments described earlier.

The ESR Spectrum of $Ag(CO)_3$. Supporting evidence for the monomeric formulation of the "green" product of the Ag–CO reaction and its dimerization to $Ag_2(CO)_6$ on warm-up has been obtained from electron spin resonance spectroscopy.

When Ag atoms were cocondensed with CO (Ag:CO $\simeq$ 1:10^4) onto a sapphire rod at 8–12 K, the ESR spectrum displayed in Figure 4 was obtained. The ESR lines continue to grow in intensity in a proportionate ratio to the amount of silver deposited, indicating their assignment to a single, paramagnetic species. Lines which could be attributed to atomic silver[15] were never observed under the conditions of these experiments.

The ESR spectrum shown in Figure 4 is typical of a molecule having axial symmetry and $S = \frac{1}{2}$. We calculate $g_\parallel$ = 2.012

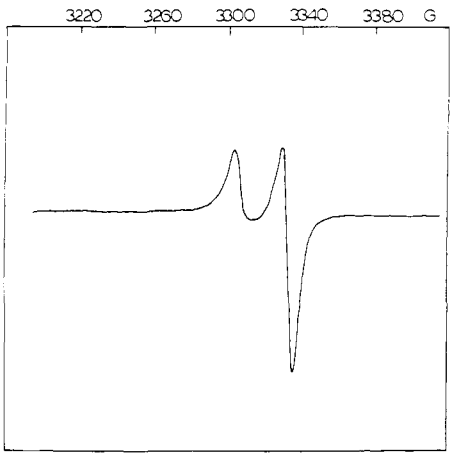

Figure 4. The ESR spectrum of the products of the matrix cocondensation reaction of silver atoms with pure CO at 10–12 K.

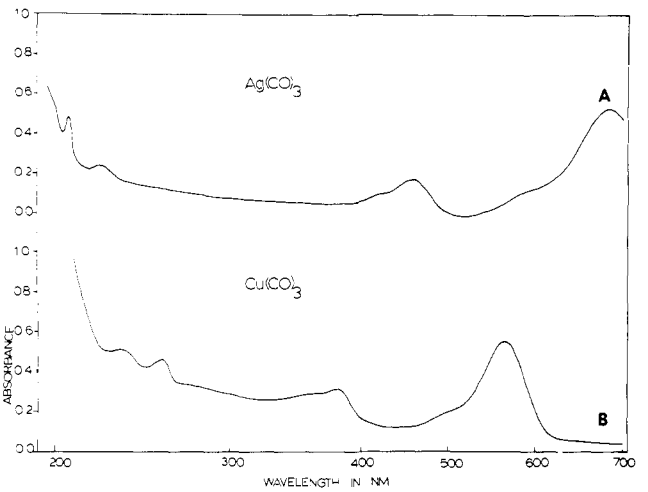

Figure 5. The uv–visible spectrum of (A) $Ag(CO)_3$ and (B) $Cu(CO)_3$ in pure CO at 10–12 K.

and $g_\perp = 1.995$. In order to qualitatively understand this relatively simple ESR spectrum, a comparison with the related data for $Cu(CO)_3$ is useful.[6]

The main features of interest for $Cu(CO)_3$ are (i) the observation of ^{63}Cu ($I = 3/2$, natural abundance 64%) and ^{65}Cu ($I = 3/2$, natural abundance 31%) hyperfine splitting, (ii) axial symmetry and $S = 1/2$, and (iii) $g_\parallel$ and $g_\perp$ close to the free electron value, 2.010 and 2.006, respectively.[6] The inherent simplicity of the related Ag/CO reaction product can be rationalized in terms of an $Ag(CO)_3$ molecule, also with axial symmetry, but with the ^{107}Ag and ^{109}Ag hyperfine splitting remaining unresolved. This is in fact quite reasonable because the nuclear magnetic moments of ^{107}Ag ($I = 1/2$, natural abundance 51%) and ^{109}Ag ($I = 1/2$, natural abundance 49%) are roughly equal but about *40* times smaller than those of the copper isotopes, and we can expect this order of magnitude difference to be reflected in the corresponding silver and copper hyperfine coupling constants. For $Cu(CO)_3$, the largest hyperfine coupling constants correspond to the perpendicular components $A_\perp$ (^{63}Cu) $\simeq$ 86 G and $A_\perp$ (^{65}Cu) = 61 G. Therefore we would expect the corresponding values for $Ag(CO)_3$ to be in the range of 2 G. As the line widths for the $g_\parallel$ and $g_\perp$ components of $Ag(CO)_3$ in pure CO are considerably larger than 2 G, it is not surprising that ^{107}Ag and ^{109}Ag hyperfine coupling remain unresolved. However, when $Ag(CO)_3$ is synthesized in dilute CO/Ar matrices, the lines are found to be considerably narrower than in pure CO, so much so that ^{107}Ag and ^{109}Ag hyperfine splitting can just be resolved. These data together with the ESR data for $Cu(CO)_3$ will be reported in detail in a forthcoming publication.[6]

Additional support for the dimerization reaction $2Ag(CO)_3 \rightarrow Ag_2(CO)_6$ in pure CO at 20–35 K stems from the observation of a monotonic decrease in the intensity of the ESR spectrum of $Ag(CO)_3$ during the annealing procedure and the nonobservation of any new ESR lines which could be ascribed to a paramagnetic intermediate. Clearly, paramagnetic $Ag(CO)_3$ is being gradually consumed to form the diamagnetic binuclear complex $Ag_2(CO)_6$.

The Uv–Visible Spectrum of $Ag(CO)_3$ and the Electronic Properties of $Cu(CO)_3$ and $Ag(CO)_3$. When $Ag(CO)_3$ was synthesized from the cocondensation reaction of Ag atoms with pure CO matrices at 8–12 K the uv–visible spectrum shown in Figure 5B and Table III was obtained. A molecular spectrum (free of Ag atoms) characterized by two very intense, broad absorptions centered at 679 and 457 nm was obtained, a situation very similar to that previously reported for $Cu(CO)_3$.[5]

In the light of the foregoing discussions, it is of considerable interest to compare the uv–visible spectrum of $Ag(CO)_3$ with

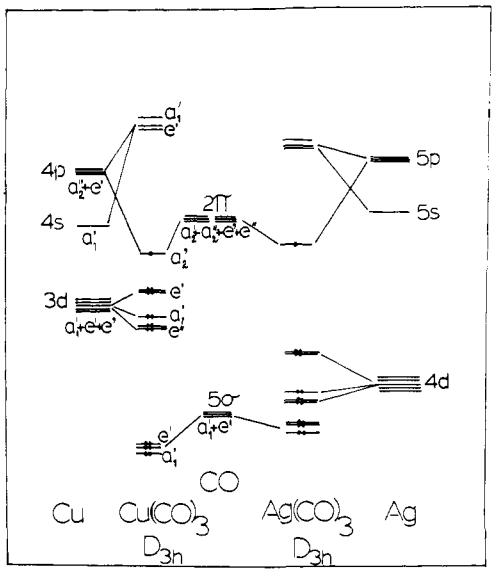

Figure 6. Qualitative molecular orbital energy level scheme for D_{3h} $Cu(CO)_3$ and $Ag(CO)_3$.

Table III. Matrix Uv-Visible Spectra for $Cu(CO)_3$ and $Ag(CO)_3$ in Solid CO

$Cu(CO)_3$[a] (nm)	$Ag(CO)_3$ (nm)	$Cu(CO)_3$[a] (nm)	$Ag(CO)_3$ (nm)
562 (s)	679 (s)	375 (ms)	457 (ms)
495 (wsh)	580 (wsh)	344 (wsh)	420 (wsh)

[a] See ref 5 for assignments of electronic transition.

that of $Cu(CO)_3$ (Figure 5A, B). The spectra are essentially shifted to lower energies compared to the corresponding ones of $Cu(CO)_3$. To interpret the above data one can make use of a qualitative comparison between the molecular orbital energy level scheme of $Cu(CO)_3$[5] and $Ag(CO)_3$ shown in Figure 6. As described previously for $Cu(CO)_3$,[5] we shall assume that the energy of the silver valence shell orbitals is approximately equal to the valence orbital ionization potentials of atomic silver[16] where the 5s and 5p levels of Ag are approximately 1000 cm^{-1} above the respective 4s and 4p levels of Cu. However, the 4d level of Ag is roughly 16 500 cm^{-1} below that of the 3d level of Cu. When account is taken of the σ and π interactions of the appropriate orbitals of Cu and Ag with the 5σ and 2π orbitals of CO, respectively, one can see that both

the σ- and π-type bonding would be expected to be slightly favored for $Cu(CO)_3$ compared to $Ag(CO)_3$. The outcome should be a greater stabilization of the highest filled π-type molecular orbital (a_2'')[17] and destabilization of the lowest empty σ- and π-type antibonding molecular orbitals for $Cu(CO)_3$ compared to $Ag(CO)_3$, the overall effect being a *red* shift of all $Ag(CO)_3$ absorptions relative to those of $Cu(CO)_3$. This prediction is found to be in qualitative agreement with the trend observed in practice (Figure 5).[18]

Another point worth mentioning at this stage is the slightly larger k_{CO} and k_{MC} bond stretching force constants for $Cu(CO)_3$ compared to $Ag(CO)_3$:

	$Cu(CO)_3$	$Ag(CO)_3$
k_{CO}	16.47	16.11
k_{MC}[19]	1.35	0.82

These force constant trends can be most easily rationalized using a proposal made recently by Fenske[20] who assumed the CO bond stretching force constants in carbonyls are linearly related to the quantity of charge donated from the 5σ orbital (σ_M) and accepted by the 2π orbital (π_M) of the CO ligand. Thus for $Cu(CO)_3$, the relationship between CO stretching force constant and σ-donated and π-accepted charge can be written:

$$k_{CO}^{Cu} = d + |a|(\sigma_{Cu} - \gamma\pi_{Cu}) \quad (I)$$

and for $Ag(CO)_3$ similarly

$$k_{CO}^{Ag} = d + |a|(\sigma_{Ag} - \gamma\pi_{Ag}) \quad (II)$$

where $|a|$, γ, and d are positive constants described previously[20] and assumed in this analysis to be approximately the same for $Cu(CO)_3$ and $Ag(CO)_3$.

We will also assume that σ_M is roughly inversely proportional to the energy separation of the 5σ on CO and the appropriate metal σ orbitals (or alternatively proportional to the Allred–Rochow electronegativities, $\chi(Cu) = 1.75$, $\chi(Ag) = 1.42$). Thus we can write

$$\sigma_{Cu} > \sigma_{Ag} \quad (III)$$

As $k_{CO}^{Cu} > k_{CO}^{Ag}$, it follows from eq I and II that

$$(\sigma_{Cu} - \gamma\pi_{Cu}) > (\sigma_{Ag} - \gamma\pi_{Ag}) \quad (IV)$$

To provide a set of circumstances which is simultaneously compatible with the two observations $k_{CuC} > k_{AgC}$ and $k_{CO}^{Cu} > k_{CO}^{Ag}$ let us consider three possibilities.

Firstly for

$$\sigma_{Cu} > \sigma_{Ag} \quad (III)$$

and

$$\pi_{Cu} > \pi_{Ag} \quad (V)$$

we require that the CO bond strengthening originating from eq III outweighs the CO bond weakening arising from (V) for $Cu(CO)_3$ compared to $Ag(CO)_3$.

Secondly, for

$$\sigma_{Cu} > \sigma_{Ag} \quad (III)$$

and

$$\pi_{Cu} < \pi_{Ag} \quad (VI)$$

we require that the CuC bond strength advantage gained from (III) outweighs the CuC bond weakening arising from (VI) for $Cu(CO)_3$ compared to $Ag(CO)_3$.

Finally, when

$$\sigma_{Cu} > \sigma_{Ag} \quad (III)$$

and

$$\pi_{Cu} = \pi_{Ag} \quad (VII)$$

we have the straightforward situation where the conditions $k_{CuC} > k_{AgC}$ and $k_{CO}^{Cu} > k_{CO}^{Ag}$ are both satisfied.

However, as k_{CO}^{Cu} is in fact only *slightly* larger than k_{CO}^{Ag} (2%) yet k_{CuC} is appreciably larger than k_{AgC} (63.5%), it would appear that the bonding situation in $Cu(CO)_3$ and $Ag(CO)_3$ is best described by

$$\sigma_{Cu} > \sigma_{Ag} \quad (III)$$

$$\pi_{Cu} \geq \pi_{Ag} \quad (V) \text{ or } (VII)$$

Silver Concentration and Diffusion Studies in Pure CO

Although the Ag/CO reaction at low silver concentrations parallels the Cu/CO reaction very closely on deposition, showing the initial formation of $Ag(CO)_3$, the dependence of the reactions on metal concentration is strikingly different in one important respect.

In the case of the Cu/CO reaction, a copper concentration study revealed that on deposition at low copper concentrations (Cu:CO $\leq$ 1:10^4) only $Cu(CO)_3$ formed whereas, on varying the Cu:CO ratio from 1:10^4 to 1:10^2, increasing concentrations of the binuclear complex $Cu_2(CO)_6$ were produced at the noticeable expense of $Cu(CO)_3$.[5]

The corresponding experiments performed with Ag/CO showed that, as the Ag:CO ratio was varied in the range 1:10^4 to 1:10^2, the only observable effect on deposition was a *decrease* in the absorbance of the $Ag(CO)_3$ but with the formation of only trace amounts of the $Ag_2(CO)_6$ complex (the latter forming readily on warming $Ag(CO)_3$ in CO at 20–35 K).[21]

The implication is that under the conditions of our cryogenic experiments and *on deposition* into pure CO, $Ag(CO)_3$ forms, which on warm-up to 25–35 K diffuses and dimerizes to $Ag_2(CO)_6$. However, at the *higher* temperatures experienced in the quasi liquid interface at the surface of the matrix during deposition (compared to the *lower* temperatures experienced within the bulk matrix during warm-up and *after deposition*) the $Ag_2(CO)_6$ preferentially decomposes, probably to small, Ag_n clusters.

Silver Dicarbonyl, $Ag(CO)_2$, in Ar, Kr, and Xe Matrices

When Ag atoms were cocondensed with dilute CO/Ar matrices (1/10 to 1/250) at 10–15 K, in addition to the 1958.2/1951.8 cm^{-1} matrix split absorption assigned previously to $Ag(CO)_3$ trapped in two slightly different sites, two other absorptions were observed in the CO stretching region at 1842.0/1827.5 cm^{-1} (Figure 2A). On deposition, the component at 1827.5 cm^{-1} was the more intense. However, during warm-up the general tendency was for the 1842.0/1827.5 cm^{-1} doublet to decrease gradually in intensity with the concomitant growth of the tricarbonyl absorption. During warm-up, the relative intensities of the 1842.0/1827.5 cm^{-1} doublet inverted, the 1842.0 cm^{-1} component being the more intense line at about 30 K. In order to identify the nature of the absorbing species giving rise to the low frequency doublet, the experiments were repeated using $^{12}C^{16}O/^{12}C^{18}O/Ar \simeq 1/1/250$ mixtures, a typical infrared spectrum being shown in Figure 2B. On deposition, the original doublet at 1842.0/1827.5 cm^{-1} in $^{12}C^{16}O/Ar$ can be seen to give rise to a "doublet of triplets" isotope pattern in the mixed isotope experiment (Figure 2B and Table IV). The intensity behavior of this isotopic spectrum during matrix warm-up shows that the triplet at 1842.0/1817.8/1799.4 cm^{-1} grows in at the gradual expense of the triplet at 1827.5/1804.0/1785.1 cm^{-1}.

These data serve to identify both components of the original 1842.0/1827.5 cm^{-1} doublet as belonging to a silver dicarbonyl molecule which, like the tricarbonyl, appears to occupy two slightly different lattice sites in CO/Ar matrices.

In order to make a structural assignment for the dicarbonyl using the infrared data alone, one is obliged to rely on the ob-

Table IV. Observed and Calculated Frequencies and Intensities of Isotopic $Ag(^{12}C^{16}O)_n(^{12}C^{18}O)_{2-n}$ or $Ag(^{12}C^{16}O)_n(^{13}C^{16}O)_{2-n}$ (where n = 0–2) in Ar, Kr, and Xe Matrices (Both Sites Included)

Obsd freq	Calcd freq	Obsd intens	Calcd intens	Assignment	
			Argon (site 2)[a]		
1799.4	1798.5	8.64	8.61	$Ag(^{12}C^{18}O)_2$	(Σ_u^+)
1817.8	1817.8	15.80	17.84	$Ag(^{12}C^{16}O)(^{12}C^{18}O)$	(A_1)
1842.0	1842.9	10.00	10.00	$Ag(^{12}C^{16}O)_2$	(Σ_u^+)
—	2010.5	0.00	0.35	$Ag(^{12}C^{16}O)(^{12}C^{18}O)$	(A_1)
			f_r = 15.20; f_{rr} = 1.48 mdyn/Å		
			Argon (site 2_1)[a]		
1785.1	1784.3	8.57	8.81	$Ag(^{12}C^{18}O)_2$	(Σ_u^+)
1804.0	1804.0	23.14	17.84	$Ag(^{12}C^{16}O)(^{12}C^{18}O)$	(A_1)
1827.5	1828.3	10.00	10.00	$Ag(^{12}C^{16}O)_2$	(Σ_u^+)
—	2046.5	0.00	0.24	$Ag(^{12}C^{16}O)(^{12}C^{18}O)$	(A_1)
			f_r = 15.40; f_{rr} = 1.89 mdyn/Å		
			Krypton (site 2)[a]		
1755.8	1755.6	8.47	8.76	$Ag(^{12}C^{18}O)_2$	(Σ_u^+)
1775.2	1775.2	16.38	17.77	$Ag(^{12}C^{16}O)(^{12}C^{18}O)$	(A_1)
1798.8	1799.0	10.00	10.00	$Ag(^{12}C^{16}O)_2$	(Σ_u^+)
—	2025.0	0.00	0.21	$Ag(^{12}C^{16}O)(^{12}C^{18}O)$	(A_1)
			f_r = 15.01; f_{rr} = 1.94		
			Krypton (site 2_1)[a]		
1747.2	1747.0	9.52	8.95	$Ag(^{12}C^{18}O)_2$	(Σ_u^+)
1766.6	1766.6	19.34	18.12	$Ag(^{12}C^{16}O)(^{12}C^{18}O)$	(A_1)
1790.0	1790.2	10.00	10.00	$Ag(^{12}C^{16}O)_2$	(Σ_u^+)
—	2038.0	0.00	0.19	$Ag(^{12}C^{16}O)(^{12}C^{18}O)$	(A_1)
			f_r = 15.05; f_{rr} = 2.11		
			Xenon (site 2)[b]		
1762.6	1762.3	9.32	8.96	$Ag(^{13}C^{16}O)_2$	(Σ_u^+)
1779.5	1779.5	20.80	17.90	$Ag(^{12}C^{16}O)(^{13}C^{16}O)$	(A_1)
1802.0	1802.3	10.00	10.00	$Ag(^{12}C^{16}O)_2$	(Σ_u^+)
—	1938.2	0.00	0.42	$Ag(^{12}C^{16}O)(^{13}C^{16}O)$	(A_1)
			f_r = 14.29; f_{rr} = 1.18 mdyn/Å		
			Xenon (site 2_1)[b]		
1750.5	1750.7	9.72	9.58	$Ag(^{13}C^{16}O)_2$	(Σ_u^+)
1768.9	1768.9	18.00	19.40	$Ag(^{12}C^{16}O)(^{13}C^{16}O)$	(A_1)
1790.8	1790.5	10.00	10.00	$Ag(^{12}C^{16}O)_2$	(Σ_u^+)
—	2032.6	0.00	0.18	$Ag(^{12}C^{16}O)(^{13}C^{16}O)$	(A_1)
			f_r = 14.99; f_{rr} = 2.04		

[a] $^{12}C^{16}O/^{12}C^{18}O$ mixtures, used with ratio ~1.07. [b] $^{12}C^{16}O/^{13}C^{16}O$ mixtures, used with ratio ~1.00.

servation or nonobservation of the high frequency, totally symmetric CO stretching mode. For a linear dicarbonyl, this mode is of course infrared inactive; however, a small distortion from linearity (5–10°) could pass undetected. Infrared spectral scans were repeatedly performed under conditions of high ordinate expansion. However, on no occasion was it possible to detect a weak line which could be assigned to the mode in question. On the basis of this negative observation, we are forced to conclude that $Ag(CO)_2$ is most probably a linear dicarbonyl.

Additional support for the dicarbonyl assignment derives from similar experiments conducted in dilute Kr and Xe matrices. In both cases, low frequency CO stretching modes are observed as doublets (1798.8/1790.0 cm^{-1} in Kr and 1802.0/1790.8 cm^{-1} in Xe) whose relative intensities change in a parallel manner to $Ag(CO)_2$ in dilute CO/Ar matrices. Mixed isotopic substitution experiments in Kr and Xe confirm the dicarbonyl assignment (Figures 3 and 7 and Table IV) for both components of the doublet for which a similar multiple trapping site interpretation seems most likely.

Isotopic frequency and intensity calculations were computed for linear silver dicarbonyl in Ar, Kr, and Xe matrices. The close agreement between the observed and calculated values shown in Table IV provides convincing support for the dicarbonyl assignment. Furthermore, the nonobservation of the in-phase high frequency mode of the mixed isotopic molecule, $Ag(^{12}C^{16}O)(^{12}C^{18}O)$ is clarified by the intensity calculations, which indicate that the intensity of this mode should be of the order of 1–2% of the intensity of the strongest component of the isotopic triplet.

Silver Monocarbonyl, AgCO, in Ar, Kr, and Xe Matrices

The monocarbonyl complex of silver proved to be a particularly difficult molecule to characterize on a number of accounts. First, and somewhat surprisingly, it turns out that it is virtually impossible to synthesize spectroscopically pure silver monocarbonyl. Even under high dilution conditions (for example, Ag:CO:Ar ≃ 0.1:1:1000) and depositions performed at 10–12 K, surface diffusion effects were sufficiently pronounced to produce interfering concentrations of the dicarbonyl and even some tricarbonyl. Second, and somewhat more problematical, was the fact that the monocarbonyl absorbs at a frequency very close to that of the tricarbonyl (which is especially pronounced in Ar where an accidental coincidence is suspected—see later). Third, if one attempts to minimize surface diffusion effects by depositing the sample at 6 K, compound formation is minimal. In order to initiate compound formation under these conditions, matrix annealing at 10–20 K is required. Unfortunately, these temperatures also favor the formation of the di- and tricarbonyl and hence the objective

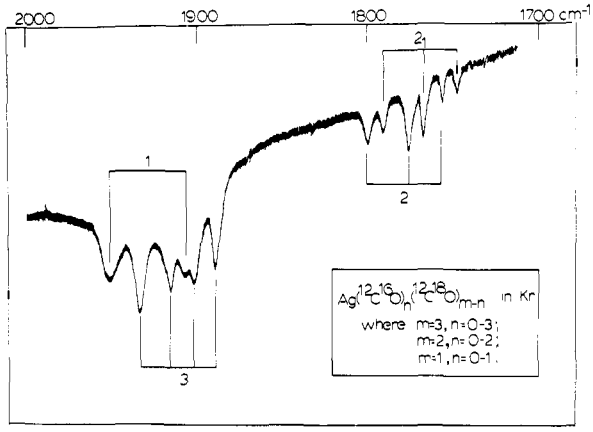

Figure 7. The matrix infrared spectrum of the products of the cocondensation reaction of Ag atoms and $^{12}C^{16}O/^{12}C^{18}O/Kr \simeq 1/1/160$ at 10–12 K after deposition where 3, 2, and 1 refer to the isotopic lines of the tri-, di-, and monocarbonyl, respectively.

Table V. Best Fit Cotton–Kraihanzel CO Bond Stretching Force Constants for $Cu(CO)_n$ and $Ag(CO)_n$ (where n = 1–3) in Argon Matrices

Complex	k_{CO}[a] (mdyn/Å)	Complex	k_{CO}[a] (mdyn/Å)
$Cu(CO)_3$	16.47	$Ag(CO)_3$	16.11
$Cu(CO)_2$	15.35	$Ag(CO)_2$	15.30
Cu(CO)	16.30	Ag(CO)	15.60

[a] Mean value quoted when two sites occur.

of the experiment, namely to obtain pure monocarbonyl, is defeated. Finally, if the experiment is performed with higher concentrations of silver, yet retaining the high dilutions of CO in Ar, the absorbances of the products decrease rather than increase, probably because of the formation of unreactive diatomic and higher aggregates of silver (discussed earlier).

The most convincing evidence for the existence of silver monocarbonyl was obtained in dilute CO/Kr and CO/Xe matrices where the tricarbonyl fortuitously experiences a larger matrix-induced red shift than the monocarbonyl and in doing so reveals the possibility of an accidental coincidence in dilute CO/Ar matrices (Figures 3 and 7). From warm-up experiments and carbon monoxide mixed isotope experiments, the monocarbonyl could be identified at 1951 cm^{-1} in Kr and 1945 cm^{-1} in Xe matrices. In actual fact, with the knowledge of a suspected accidental coincidence for AgCO and $Ag(CO)_3$ in Ar matrices, a careful reexamination of the warm-up behavior of the infrared spectra and the mixed isotope experiments discloses subtle intensity anomalies, indicative of the presence of more than a single species absorbing at the tricarbonyl frequency. We therefore tentatively assign the monocarbonyl at 1958 cm^{-1} in Ar matrices.

The Anomalous C.K. CO Bond Stretching Force Constant Trends for $M(CO)_n$ (where M = Cu or Ag; n = 1–3)

The discovery of thermally unstable carbonyls of copper and silver can be considered to add a new dimension to our knowledge of binary carbonyls of the transition metals. Historically speaking, the data for copper authenticate some of the very early claims[23] for unstable copper carbonyls which were postulated to exist in the vapors of copper transported by streams of heated CO. Clearly, the generally held view for the nonexistence of copper and silver carbonyls, namely the stability of the nd^{10} valence shells, is no longer tenable in view of their apparently "normal" CO stretching frequencies (2050–1800 cm^{-1}, cf. $Ni(CO)_4$, ν(CO) (T_2) 2050 cm^{-1}).

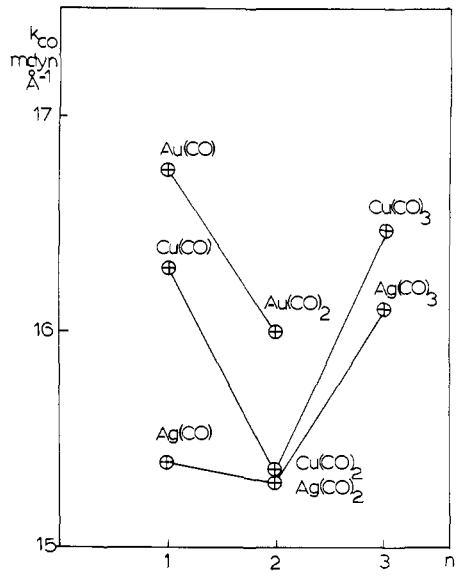

Figure 8. Graphical representation of the C.K. CO bond stretching force constants for $Cu(CO)_n$ and $Ag(CO)_n$ (where n = 1–3) as a function of n. $Au(CO)_n$ (where n = 1–2) have been included for comparison[7].

Clearly these results indicate a considerable degree of charge delocalization from the metal onto the CO ligand. Note, however, that the metal–carbon stretching frequencies (ν(Cu–C), 375–325 cm^{-1} and ν(Ag–C) = 250 cm^{-1}) are quite low and imply a weaker M–C interaction than for $Ni(CO)_4$ (ν(NiC) (T_2), 438 cm^{-1}) consistent with the lower thermal stabilities of $Cu(CO)_n$ and $Ag(CO)_n$ (where n = 1–3).

In this discussion we shall show how the "anomalous" trend observed in the C.K. CO force constants for $M(CO)_n$ (where M = Cu or Ag; n = 1–3) can be fitted into a logical bonding scheme.

We have used the term "anomalous" to emphasize a striking difference between the group 1b binary carbonyls and those of Ni,[29] Pd,[24,25] Pt,[26] Co,[27] Rh,[28] or Ir,[28] namely an *amonotonic* trend in the C.K. CO stretching force constants (Figure 8, Table V) for the former, that is:

$$Cu(CO)_3 > Cu(CO) > Cu(CO)_2 \quad \text{(ref 5)}$$

$$Ag(CO)_3 > Ag(CO) > Ag(CO)_2 \quad \text{(this study)}$$

$$Au(CO) > Au(CO)_2 \quad \text{(ref 27)}$$

yet a consistently *monotonic* trend for the latter, for example,

$$Co(CO)_4 > Co(CO)_3 > Co(CO)_2 > Co(CO) \quad \text{(ref 27)}$$

$$Pt(CO)_4 > Pt(CO)_3 > Pt(CO)_2 > Pt(CO) \quad \text{(ref 26)}$$

The rationalization used to explain the normal trend for the binary carbonyls of the nickel and cobalt groups involves the synergic relationship between the 5σ and 2π orbital contributions to the bonding of the CO ligand to the metal. Thus, as the coordination number increases, the extent of charge delocalization from the metal to the CO, per ligand, decreases. As this charge mainly enters the 2π antibonding orbitals on CO, the effect is a strengthening of the carbon–oxygen bond with increasing n. On the other hand, the σ charge donation from the 5σ orbital on CO to the metal is expected, if anything, either to remain roughly constant or decrease per ligand as n increases. As the 5σ orbital on CO is slightly antibonding, the effect should be a slight weakening of the carbon–oxygen bond with increasing n. From the observation of increasing k_{CO} with n in the series $M(CO)_n$ (where M = Ni, Pd, Pt, Co, Rh, or Ir[24–29]), one must conclude that the decreasing 2π orbital population on CO predominates over the decreasing (or constant) 5σ orbital population.

Two assumptions are necessary to explain the amonotonic behavior of the group 1b binary carbonyls (Figure 8, Table V). First, π back-bonding effects from the stable valence d orbitals to the 2π orbitals of CO are minimal (if any contribution at all, the effect will be greater for Cu than Ag). Second, the charge density on the metal remains roughly constant with coordination number n and so the valence d-orbital stabilities are little affected as n changes.

Let us consider each molecule in turn.

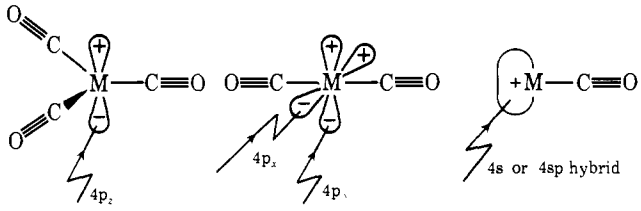

In view of the decreasing ^{63}Cu, ^{65}Cu hyperfine coupling constants on passing from Cu(CO) to $Cu(CO)_3$,[6] one can conclude that the 4s character of the odd electron is decreasing in the same order. In fact, an analysis of the ESR data for Cu(CO) indicates that the odd electron is almost entirely localized in a pure 4s orbital.[6] On the other hand, the ESR data for $Cu(CO)_3$ are consistent with a $^2A_2''$ electronic ground state with the odd electron in a copper $4p_z$ orbital, largely delocalized into the π molecular orbital system of the three CO ligands.[6]

The implications are that we can describe the σ-bonding scheme for the tricarbonyl as approximately sp^2 with π-bonding to the CO through the $4p_z$ orbital containing the odd electron. Similarly we can describe the σ-bonding scheme of the dicarbonyl as approximately sp with π-bonding to the CO through the $4p_x$, $4p_y$ degenerate set containing the odd electron. Hence the tricarbonyls and dicarbonyls should display the "normal" trend in the C.K. CO stretching force constants, as the π- and σ-charge transfer per CO group should decrease as n increases, that is, $Cu(CO)_3 > Cu(CO)_2$ and $Ag(CO)_3 > Ag(CO)_2$ as observed.

However, the monocarbonyl is unique in one important respect, namely the electronic ground state is $^2\Sigma^+$, having the odd electron in a σ-type orbital, in contrast to the π-character of the odd electron in the tri- and dicarbonyl.

The so-called "anomaly" can now be reconciled, as the π-contribution to the M–C bond of the monocarbonyl, instead of being the largest, turns out to be the smallest in the series. Moreover, the σ-contribution gains in importance in the monocarbonyl with the result that the C.K. CO stretching constant is higher than anticipated and the *amonotonic* order results. (Clearly some $d\pi-\pi^*$ bonding occurs, as the monocarbonyl absorbs below the frequency of free CO.) This rationale would appear to hold generally for the carbonyls of Cu, Ag, and Au (Figure 8).

The Relationship between CuCO and AgCO and Carbon Monoxide Chemisorbed onto Cu and Ag Metallic Films. Three features of the infrared spectra of CO chemisorbed onto Cu and Ag metallic films are worth mentioning.[2] First, only terminally bonded CO groups are observed. Second, they absorb at frequencies very close to that of gaseous CO (2138 cm^{-1}), and third, the frequencies for CO chemisorbed on Cu and Ag are very similar: CuCO, 2010 (ref 5); $CuCO_{chemi}$, 2100 (ref 2); AgCO, 1958 (this study); $AgCO_{chemi}$ 2119 (ref 2). As described in the previous section, π-bonding effects in CuCO and AgCO from the unpaired electron are symmetry forbidden and only minimal π-contributions from the 3d or 4d valence shells are anticipated.

Clearly in the case of CO chemisorbed onto Cu or Ag this description still applies but with the added restriction that the π-effects are expected to be even *less* pronounced because of the participation of the valence d electrons in the band structure of the metal. Hence the predominant bonding contribution for CO chemisorbed onto Cu and Ag is of a σ-type with minimal π back-donation, sufficient only to lower the CO stretching frequency slightly below that of free CO.

The Importance of p Orbitals in the π-Bonding Schemes of Metal Carbonyls

In a sense, the discussions of the previous sections have led us naturally into the subject of p_π contributions to the overall bonding scheme and stability of metal carbonyl complexes. This topic is especially interesting in view of the synthesis of Ga,[30] Ge, and Sn[31] carbonyls which have one thing in common with the group 1b carbonyls, namely a stable, filled valence d shell. The synthesis of Al carbonyls[32] adds a further dimension to this discussion, namely how to assess the bonding scheme of a carbonyl complex whose central metal atom is devoid of valence d electrons.

It would seem not to be too unreasonable to extend the bonding ideas expounded for the group 1b carbonyls to the main group carbonyl complexes $Al_x(CO)_2$, $Ga_x(CO)_2$, $Ge(CO)_n$, and $Sn(CO)_m$. We therefore suggest that similar $p\pi-\pi^*$ bonding with minimal $d_\pi-\pi^*$ contributions (impossible of course for Al) furnish sufficient stabilization to give these main group carbonyls an independent existence.

In view of the facile matrix surface diffusion and dimerization of light metal atoms, the aluminum and gallium dicarbonyl complexes are probably best formulated $Al_2(CO)_2$[33] and $Ga_2(CO)_2$. The aluminum complex is especially interesting. Whether it is formulated as I or II below, the main

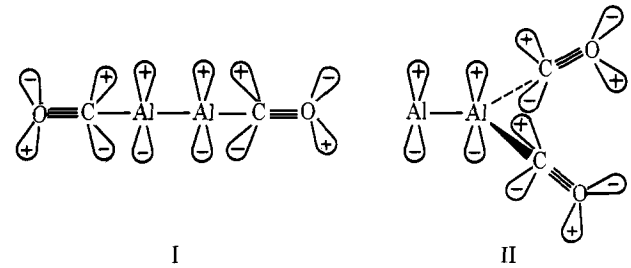

I II

π-contribution to the Al–C bonding scheme is $p_\pi-\pi^*$.

Matrix-Induced Vibrational Frequency Shifts for $Ag(CO)_n$ (where n = 1–3). A study of vibrational frequency shifts for molecules in various solvents can sometimes provide useful information as to the nature of the solute–solvent interaction and as such can distinguish nonspecific interactions from weak chemical bonds. The theoretical interpretations of solute–solvent interactions have more recently been extended to include guest–host interactions for molecules, radicals, and ions trapped in solid matrices.[35] However, the detailed interpretation of a vibrational frequency shift from the gas phase to the matrix, defined as $\Delta\nu = \nu_{gas} - \nu_{matrix}$, is a complex calculation even for the simplest of systems and makes quantitative evaluation of matrix shifts impracticable. Providing the guest molecule is trapped within a "flexible" matrix cage, one would not expect its frequency shift behavior to differ markedly from the molecule in solution, in the case of nonspecific guest–host interactions. Let us apply the Buckingham equation[36]

$$\frac{\Delta\nu}{\nu} = C_1 + \tfrac{1}{2}(C_2 + C_3)\left(\frac{\epsilon' - 1}{2\epsilon' + 1}\right)$$

which has been used with some success to explain nonspecific solvent shifts in $Co(CO)_n$ (where n = 1–4),[27] to the case of $Ag(CO)_n$ (where n = 1–3) in various matrices.

The binary carbonyls of silver have been studied in Ar, Kr, and Xe and in the case of $Ag(CO)_3$ and Ag(CO) show a monotonic red shift (a loose cage environment according to Pimentel and Charles[37]) on passing from Ar to Kr to Xe ma-

Table VI. Buckingham Frequency Plots for Ag(CO) and $Ag(CO)_3$ in Ar, Kr, and Xe Matrices

		ν_{matrix}	$\Delta\nu$	$(\Delta\nu/\nu) \times 10^{-2}$ [b]	$(\epsilon' - 1)/(2\epsilon' + 1)$ [c]
$Ag(CO)_3$	Ar	1955.0	20.0	1.02	0.148
	Kr	1932.8	42.2	2.16	0.185
	Xe	1926.3	48.7	2.50	0.221
	Gas[a]	1975.0			
Ag(CO)	Ar	1958.0	8.0	0.41	0.148
	Kr	1951.0	15.0	0.76	0.185
	Xe	1945.0	21.0	1.08	0.221
	Gas[a]	1966.0			

[a] Extrapolated value. [b] ν is the arithmetic mean frequency observed for the complex in the matrix and gas phase. [c] $\epsilon'_{20K} = 2.19$ (Xe), 1.88 (Kr), and 1.63 (Ar).

trices.[38] Especially noteworthy is the amonotonic frequency trend for $Ag(CO)_2$ (Tables I, IV). The matrix frequencies for $Ag(CO)_3$ and Ag(CO) in fact show an approximately linear dependence on the matrix polarizability, and extrapolation to zero polarizability yields the frequencies 1975 and 1966 cm^{-1}, respectively. We shall refer to these values as ν_{gas}, the "pseudo-gas-phase frequencies" for $Ag(CO)_3$ and Ag(CO), respectively. Using these ν_{gas} values, one can determine the Buckingham frequency shift ratio $\Delta\nu/\nu$ (where ν is taken as the arithmetic mean of ν_{gas} and ν_{matrix}). The $\Delta\nu/\nu$ values are listed in Table VI and, when plotted against $(\epsilon' - 1)/(2\epsilon' + 1)$, show a roughly linear dependence for Ar, Kr, and Xe (the data could only be tested for these matrices, because of limited ϵ' (20 K) data available for solid-state "gases").

Although the results are not extensive, it would appear that $Ag(CO)_3$ and Ag(CO) interact in a nonspecific manner with noble gas matrices. However, the data for $Ag(CO)_2$ seem to be anomalous in this respect, showing erratic frequency shifts in Ar, Kr, and Xe matrices. It is not inconceivable that $Ag(CO)_2$ in Xe (whose asymmetric CO stretching mode appears most out of line) is slightly distorted away from linearity, possibly because of a weak interaction with the Xe in its vacant coordination site.

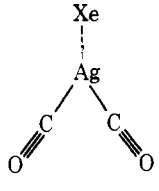

A distortion of this type would in fact be most pronounced for $Ag(CO)_2$ and might pass unnoticed for $Ag(CO)_3$ and Ag(CO). In this context we note that weak chemical bonds of this type have been recently proposed for $Xe\cdots Fe(CO)_4$[39] and $Xe\cdots Cr(CO)_5$.[40]

Acknowledgments. We would like to thank the National Research Council of Canada, the Research Corporation, and the Atkinson Foundation for financial assistance, and the National Research Council for a scholarship for D.M.

References and Notes

(1) T. Graham, *Philos. Trans. R. Soc. London*, **156**, 399 (1866); W. Stahl, *Chem.-Ztg.*, **39**, 885 (1915); W. Mauchot, T. König, and H. Gall, *ibid.*, **57**, 1157 (1924).
(2) J. Pritchard and M. L. Sims, *Trans. Faraday Soc.*, **59**, 437 (1963); **56**, 427 (1970); R. Greenler, private communication.
(3) E. P. Kündig and G. A. Ozin, *Prog. Inorg. Chem.* (1974).
(4) J. S. Ogden, *Chem. Commun.*, 978 (1971).
(5) H. Huber, E. P. Kündig, M. Moskovits, and G. A. Ozin, *J. Am. Chem. Soc.*, **97**, 2097 (1975).
(6) E. P. Kündig, D. McIntosh, B. McGarvey, and G. A. Ozin, unpublished work.
(7) D. McIntosh and G. A. Ozin, *Inorg. Chem.*, (in press).
(8) E. P. Kündig, M. Moskovits, and G. A. Ozin, *J. Mol. Struct.*, **14**, 137 (1972).
(9) M. Moskovits and G. A. Ozin, *Appl. Spectrosc.*, **26**, 481 (1972).
(10) L. A. Hanlan and G. A. Ozin, *J. Am. Chem. Soc.*, **96**, 6324 (1974).
(11) H. Huber and G. A. Ozin, unpublished work.
(12) M. Ackerman, F. E. Stafford, and J. Drowart, *J. Chem. Phys.*, **33**, 1784 (1960), and references therein.
(13) A small splitting (1958.2/1951.8 cm^{-1}) was observed in Ar and is shown later on to be a multiple trapping site effect.
(14) F. A. Cotton and C. S. Kraihanzel, *J. Am. Chem. Soc.*, **84**, 4432 (1962).
(15) P. Kasai and D. McLeod, Jr., *J. Chem. Phys.*, **55**, 1566 (1971).
(16) I. Baranovskii and A. B. Nikolskii, *Teor. Eksp. Khim.*, **3**, 527 (1967).
(17) The electronic ground state of $Cu(CO)_3$ has been shown by ESR spectroscopy to be $^2A_2''$.[6]
(18) Extended Hückel molecular orbital calculations[6] for $Cu(CO)_3$ and $Ag(CO)_3$ yield energy level schemes which are in good agreement with those shown in Figure 5.
(19) The k_{MC} force constants were calculated using a method similar to that described in E. P. Kündig, D. McIntosh, M. Moskovits, and G. A. Ozin, *J. Am. Chem. Soc.*, **95**, 7234 (1973), except that $k_{MC,MC} = 0.1k_{MC}$.
(20) M. B. Hall and R. F. Fenske, *Inorg. Chem.*, **11**, 1619 (1972).
(21) In this context, it is important to note that the uv–visible spectrum of Ag atoms deposited into Ar under comparable concentration conditions to those described for CO (1:10^4 to 1:10^2) shows, besides Ag atoms, *appreciable* concentrations of a species which has been identified as disilver, Ag_2.[22]
(22) G. A. Ozin, *Appl. Spectrosc.*, (in press).
(23) M. I. Bruce, *J. Organomet. Chem.*, **44**, 209 (1972).
(24) E. P. Kündig, M. Moskovits, and G. A. Ozin, *Can. J. Chem.*, **50**, 3587 (1972).
(25) J. H. Darling and J. S. Ogden, *Inorg. Chem.*, **11**, 666 (1972).
(26) E. P. Kündig, D. McIntosh, M. Moskovits, and G. A. Ozin, *J. Am. Chem. Soc.*, **95**, 7234 (1973).
(27) L. Hanlan, H. Huber, E. P. Kündig, B. McGarvey, and G. A. Ozin, *J. Am. Chem. Soc.*, **97**, 7054 (1975).
(28) L. Hanlan and G. A. Ozin (unpublished work).
(29) R. Dekock, *Inorg. Chem.*, **10**, 1205 (1971).
(30) J. S. Ogden in "Cryochemistry", G. A. Ozin and M. Moskovits, Ed., Wiley, New York, N.Y., 1975.
(31) A. Bos, *J. Chem. Soc., Chem. Commun.*, 26 (1972).
(32) A. J. Hinchcliffe, J. S. Ogden, and D. D. Oswald, *J. Chem. Soc., Chem. Commun.*, 338 (1972).
(33) The binuclear formulation for $Al_2(CO)_2$ would seem to be quite reasonable in the light of recent matrix uv–visible Al/Ar metal concentration experiments which provide evidence for the formation of substantial amounts of Al_2 on deposition.[34] Al/CO concentration experiments will be required to verify this proposal.
(34) D. Gruen, private communication.
(35) A. J. Barnes in "Vibrational Spectra of Trapped Species", H. Hallam, Ed., Wiley, London, 1973.
(36) A. D. Buckingham, *Proc. R. Soc. London, Ser. A*, **248**, 169 (1958); **255**, 32 (1960); *Trans. Faraday Soc.*, **56**, 753 (1960).
(37) G. C. Pimentel and S. W. Charles, *Pure Appl. Chem.*, **7**, 111 (1963).
(38) When the molecule appears in two matrix sites (see tables), the mean frequency was used for the polarizability (α, $Å^3$) frequency (cm^{-1}) plots.
(39) J. J. Turner and M. Poliakoff, *J. Chem. Soc., Dalton Trans.*, 2276 (1974).
(40) J. J. Turner and R. N. Perutz, private communication and *J. Am. Chem. Soc.*, in press.
(41) D. McIntosh, M. Moskovits, and G. A. Ozin, *Inorg. Chem.*, (in press).